Molecular association between water and dimethyl sulfoxide in solution: A molecular dynamics simulation study

Ivana A. Borin and Munir S. Skaf

Citation: The Journal of Chemical Physics **110**, 6412 (1999); doi: 10.1063/1.478544

View online: http://dx.doi.org/10.1063/1.478544

View Table of Contents: http://scitation.aip.org/content/aip/journal/jcp/110/13?ver=pdfcov

Published by the AIP Publishing

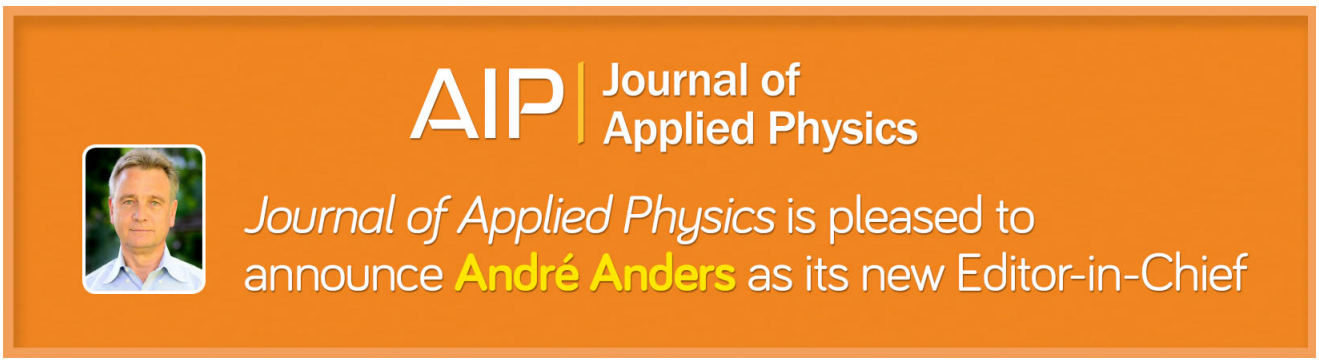

Molecular association between water and dimethyl sulfoxide in solution: A molecular dynamics simulation study

Ivana A. Borin and Munir S. Skaf
Instituto de Química, Universidade Estadual de Campinas, Cx. P. 6154, Campinas, SP, 13083-970, Brazil

(Received 22 June 1998; accepted 9 December 1998)

A molecular dynamics simulation study of the local structures and H-bond distribution for water–dimethyl sulfoxide (DMSO) mixtures over the entire composition range is presented. Analysis of several site-site pair distribution functions reveals that two well-defined kinds of aggregates characterize the molecular association between water and DMSO in solution. One of them, already identified through recent neutron diffraction experiments and computer simulations, consists of two water molecules H-bonded to the oxygen atom of a DMSO molecule, such that the angle between the two H-bonds is nearly tetrahedral. The other complex features a central water molecule and two DMSO, making H-bonds to water hydrogens. According to the simulation data, these molecular aggregates coexist with each other in the mixture, but their proportions change with composition. 1DMSO-2water complexes predominate over 2DMSO-1water aggregates for water-rich mixtures (water mole fractions $>50\%$), whereas the opposite is true for DMSO-rich mixtures. The present simulations also seem to indicate that an association between a pair of DMSO molecules through their oxygen atoms is made possible by the formation of the 2DMSO-1water complexes. Implications of the existence of these aggregates to the mobility and other dynamic properties of these mixtures are briefly discussed. © *1999 American Institute of Physics.*
[S0021-9606(99)50511-4]

I. INTRODUCTION

Excess physicochemical properties of dimethyl sulfoxide (DMSO)–water mixtures present strong deviations from ideality, with maximum deviation occurring around 30% to 40% mole fraction of DMSO.[1–4] Examples of highly nonideal mixing behavior are found in measurements of dielectric constants, NMR relaxation times, viscosity, density, and heat of mixing, amongst others. Such strong deviations from the ideal mixing behavior have often been attributed to the formation of 1DMSO-2H_2O molecular aggregates, where two water molecules are supposedly tightly hydrogen (H)-bonded to the oxygen atom of a DMSO molecule. According to this interpretation, extrema of excess quantities would then be likely found at DMSO mole fraction $x_D \approx 0.33$. Although the existence of well-defined 1DMSO-2water complexes in these mixtures has not been conclusively established in the literature, neutron diffraction data suggest that DMSO-water complexes do exist at that composition.[5] The question as to whether such H-bonded aggregates are actually long-lived complexes is more controversial since available experimental results do not provide sufficiently detailed information in this regard.

Another important and closely related aspect concerns the extent over which DMSO affects the structure of water in the mixture. In this respect, the recent neutron diffraction experiments[5] have shown that the local tetrahedral order of water in these mixtures is preserved even at high ($x_D \approx 0.35$) concentrations of DMSO. This has been confirmed by means of molecular dynamics (MD) simulations as well.[6]

To our knowledge, several MD simulation studies have been reported in the literature aimed at the structure,[5(b)–8] H-bond distribution,[5(b)–7] and H-bond dynamics[9] of DMSO–water mixtures. These studies have focused on water-rich mixtures. Vaisman and Berkowitz[7] simulated diluted mixtures ($x_D = 0.005$, 0.04, and 0.2), focusing on the local structure of water upon addition of DMSO and on the H-bonding distribution between the two constituents. Their simulations show the existence of 1DMSO-2water H-bonded aggregates at the three compositions studied. Using different force fields, Luzar and Chandler[6] performed MD simulations at two compositions ($x_D = 0.21$ and 0.35), focusing on the structural properties, H-bond distribution, and H-bond dynamics. Their simulations reveal several important aspects of these mixtures; three of them are worth mentioning here: First, they show that the local tetrahedral order of water molecules is preserved even for the concentrated ($x_D = 0.35$) solution, in agreement with previous neutron diffraction data.[5] Second, they show that, at the compositions studied, DMSO acts typically as a double H-bond acceptor, forming 1DMSO-2water H-bonded aggregates of nearly tetrahedral geometry. Third, their analyses of the H-bond lifetimes indicate that DMSO–water H-bonds are longer lived than water–water H-bonds in the mixture, which in turn are longer lived than in neat water. In a more recent work, which combined neutron scattering and computer simulations, Soper and Luzar[8] have found no evidence of hydrophobic association of DMSO and that the enhanced correlations presented by water in these mixtures are due to the strong H-bonding of water to the oxygen atom of DMSO.

While great progress has been made toward obtaining an accurate molecular level understanding of DMSO–water mixtures on the water-rich side, mixtures rich in DMSO,

where water plays the role of solute, have not been explored from a microscopic point of view. We feel that further work is needed in order to characterize the molecular behavior of these mixtures in a more complete way. In particular, very little is known about way the mixture's intermolecular structure evolves with increasing concentration of DMSO, what the local structures and H-bonding distributions for DMSO-rich mixtures are, and also, how does transport associated with each molecular species and other dynamical properties behave as a function of composition? To answer these and other equally important questions, we have undertaken a series of MD simulations of DMSO–water mixtures spanning the whole composition range. In this paper, we focus on the intermolecular structure given in terms of site-site pair distribution functions, and the distribution of water–water and water–DMSO H-bonds for mixtures of different compositions. We show in particular that, according to the simulations, a distinct type of molecular aggregate, namely, one consisting of two DMSO molecules H-bonded to the hydrogen atoms of a central water molecule, is expected to be the predominant form of molecular association between water and DMSO in DMSO-rich mixtures. Some results are also presented for the diffusion coefficients and the single-particle reorientational relaxation times. A more detailed study of the dynamics, dipole orientational correlations, and dielectric properties shall be reported separately.

The remainder of the paper is organized as follows: The next section describes the intermolecular potentials and technical details of the simulations. In Sec. III, we present and discuss our results for the mixtures' internal energy and intermolecular structure on the basis of various site-site pair distribution functions. We shall see how the structure of DMSO changes upon mixing with water, and how DMSO affects the structure of water, extending to higher DMSO concentrations some of the analysis reported in previous works. Also in Sec. III, we discuss the distribution of H-bonds involving water–water and water–DMSO pairs, as well as the single-particle dynamics as functions of composition. Our concluding remarks are presented in Sec. IV.

II. INTERACTION POTENTIALS AND SIMULATION DETAILS

We have considered here mixtures with DMSO mole fractions $x_D = 0.13$, 0.35, 0.50, 0.66, and 0.81, as well as the pure liquids at ambient conditions. For water we have used the well-known SCP/E model,[10] while for DMSO we used the four-site $P2$ potential of Luzar and Chandler,[6] where the methyl groups are treated as united atoms. There is no particular reason for this choice of potentials. We have based our choice essentially on three general aspects: First, both the SPC/E and $P2$ are very simple models which describe reasonably well the thermodynamics, the structure, and some dynamical properties of water (see, for instance, Ref. 11) and DMSO.[5,6,9,12] Second, we have shown[12] that among the available force fields for DMSO,[6,13–15] the ones which best describe the real liquid, including its static dielectric behavior, are Luzar and Chandler's $P2$,[6] Jörgensen's OPLS,[14] and the model parametrized by Liu *et al.*[15] Third, previous simulations[6] have shown that for some compositions, the mixture's thermodynamics and, to some extent, the intermolecular structure, are not strongly dependent on the DMSO force field. Thus, one could, in principle, have used other existing potentials for DMSO, or water for that matter, to study these mixtures to the same level of reliability. Despite that, we shall see below that the interactions between DMSO and water in the present simulations may be somewhat overestimated compared to the real mixture.

Both SPC/E and $P2$ are rigid, nonpolarizable intermolecular potentials whose site-site interactions are given by a sum of Lennard-Jones plus Coulomb terms,

$$V_{ij}(r) = 4\varepsilon_{ij}\left[\left(\frac{\sigma_{ij}}{r}\right)^{12} - \left(\frac{\sigma_{ij}}{r}\right)^{6}\right] + \frac{q_i q_j}{4\pi\varepsilon_0 r}, \tag{1}$$

where q_i is the partial charge on site i, ε_{ij} and σ_{ij} are the Lennard-Jones interaction parameters between sites i and j on distinct molecules, and r the separation between these sites. The Lennard-Jones interaction parameters between sites of different types are set by the usual Lorentz-Berthelot combining rules, $\varepsilon_{ij} = \sqrt{\varepsilon_{ii}\varepsilon_{jj}}$ and $\sigma_{ij} = (\sigma_{ii} + \sigma_{jj})/2$. This procedure has been used in other simulations of aqueous mixtures, including DMSO–water mixtures, with apparent success. Site parameter and molecular geometries for the simulated models are found in Refs. 6 (DMSO) and 10 (water).

The simulations have been performed on the NVE ensemble with 864 molecules placed in cubic boxes with periodic boundary conditions at an average temperature of 298 K. The numbers of DMSO molecules corresponding to the mixtures at 13%, 35%, 50%, 66%, and 81% of DMSO are 115, 302, 432, 574, and 703, respectively. The pure water simulations were run using 256 molecules. In each case, the box dimensions were chosen so as to match the corresponding experimental densities[1] at 298 K and 1 atm. During the simulations, the Lennard-Jones forces were cut off at half the box length, while Ewald sums with conducting boundaries[16] were applied to the long-ranged portions of the electrostatic forces. The equations of motion were integrated using the leapfrog[17] algorithm with a time step of 4 fs, while the molecular geometries were restored using SHAKE.[18] This enabled total energy conservation within 0.1% error during uninterrupted production runs lasting about 20 ps for each mixture. We performed about four 20 ps production runs for each state. These runs were separated by smaller (4 ps) runs during which the velocities were rescaled according to the desired temperature. Before the production runs, each mixture was equilibrated during 40-60 ps starting from a face-centered-cubic (fcc) lattice over which water and DMSO molecules were randomly distributed. Water and DMSO density profiles were also calculated after equilibration to ensure the system is homogeneous throughout.

III. RESULTS AND DISCUSSION

The main focus of this work is on the local structures presented by water and DMSO and how these structures change with composition. However, before discussing that, it is important to show some of the thermodynamic behavior exhibited by these mixtures. In Table I, we show the mean

TABLE I. Average potential energy (U), pressure (p), and half the box length ($L/2$) for each simulated mixture. The experimental potential energy ($U^{\exp} \approx -\Delta H_{\text{vap}} + RT$) is estimated from the mixture's enthalpy of vaporization (Refs. 1 and 19), $\Delta H_{\text{vap}} = x_D \Delta H^D_{\text{vap}} + x_W \Delta H^W_{\text{vap}} \Delta H_{\text{mix}}$.

Mole fraction of DMSO	$-U$ (kJ/mol)[a]	p (kbar)	$L/2$ (Å)[b]	$-U^{\exp}$ (kJ/mol)
0.00	41.4	0.20 ± 1.1	9.86	41.5
0.13	45.1	0.04 ± 0.5	16.42	44.6
0.35	49.6	-0.15 ± 0.4	18.57	47.5
0.50	50.7	-0.32 ± 0.5	19.87	48.6
0.66	50.6	0.07 ± 0.5	21.15	49.3
0.81	49.8	-0.11 ± 0.3	22.19	49.8
1.00	49.1	-0.18 ± 0.5	23.34	50.4

[a]Estimated error for the simulated average potential energy is ± 0.15 kJ/mol.
[b]For pure water we used $N=256$ molecules. For pure DMSO and all mixtures we used $N=864$.

potential energy per mole (U), the pressure (p), and (half) the length of the simulation box ($L/2$) for each simulation stated. Despite the large fluctuations, the simulations yield vanishing pressure within the error bars, as they should. The mean potential energy compares well with the estimated experimental internal energy, $U^{\exp}$, which has been obtained from the experimental vaporization heats of the pure liquids[19] and the excess heat of mixing[1,2] according to $U^{\exp} \approx -\Delta H_{\text{vap}} + RT$, where $\Delta H_{\text{vap}} = x_D \Delta H^D_{\text{vap}} + x_W \Delta H^W_{\text{vap}} - \Delta H_{\text{mix}}$. One notices, however, that unlike $U^{\exp}$, the simulated internal energy passes through a minimum around 50% or 66% mole fraction of DMSO. Table I also reveals that the potentials used slightly overestimate the intermolecular interactions in the mixed solvents.

Perhaps the most interesting thermodynamic property to be evaluated from computer simulations is the enthalpy of mixing, since this quantity has been experimentally measured at several compositions.[1–3] However, in order to calculate the enthalpy or free energy of mixing, it would require simulating in the NpT ensemble or going through a thermodynamic perturbation scheme which is a computationally costly and more demanding procedure. Fortunately, the excess internal energy as a function of composition also provides a convenient means of discussing the simulated thermodynamic data. The results are displayed in Fig. 1 (circles; left axis), along with the experimental enthalpy of mixing from Fox and Whittingham[2] (triangles; right axis). Both quantities are negative over the whole composition range, with minima around 40% mole of DMSO, which is indicative of the strong H-bonding interactions between DMSO and water that govern the bulk and interfacial thermodynamic behavior of these mixtures.[20] The excess internal energy and the enthalpy of mixing should be very close to each other since they differ by pV^{ex}, which is indeed very small ($\sim 10^{-4}$ kJ/mol or less) over the entire composition range. However, Fig. 1 shows a factor of two between the simulated excess energy and the experimental enthalpy of mixing. In absolute values, the difference between the simulated and experimental excess quantities is ~ 3 kJ/mol at most. A closer inspection of Table I reveals that this difference stems precisely from the mismatch between U and $U^{\exp}$, that is, from the fact that the mixture's internal energy as given by the simulations is slightly overestimated. While the SPC/E and $P2$ potentials have been parametrized to reproduce the pure liquids' enthalpy of vaporization, no further readjusment has been made for the mixtures. Figure 1 shows, then, that a small composition-dependent adjustment in the potential parameters for cross-species is necessary in order to describe the real mixture's heat of mixing more accurately.

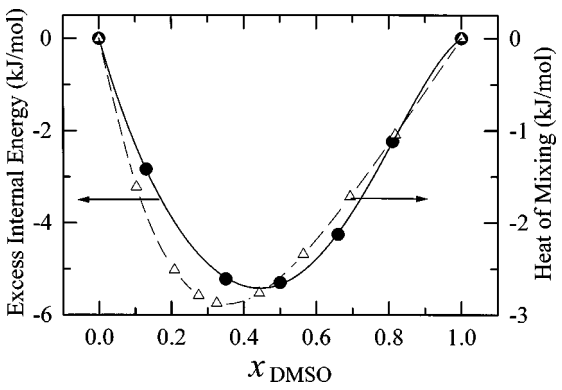

FIG. 1. The simulated excess internal energy (circles, left axis) and the experimental enthalpy of mixing from Ref. 2 (triangles, right axis) as functions of composition. The lines are just guides to the eye.

It is not a simple matter to establish one-to-one correspondence between the thermodynamic and other bulk properties with the microscopic nature of the liquid. Nevertheless, detailed molecular level information about the way molecules associate with each other in the liquid can be gained by means of computer simulations. One of the most useful ways of investigating the intermolecular structure of liquids from neutron scattering or x-ray diffraction data and computer simulations consists of the analysis of the site-site pair distribution functions, $g_{\alpha\beta}(r)$. In our case, each simulated mixture has as many as 15 distinct site-site functions involving water–water, DMSO–water, and DMSO–DMSO site pairs. We find, however, that a smaller subset of pair distributions is able to capture the general aspects of the mixtures' structure and, in particular, also yields a sufficiently detailed picture of the local order of DMSO and water molecules.

A. DMSO-DMSO pair distributions

We begin by looking at the DMSO–DMSO $g_{\alpha\beta}(r)$ functions involving the SS, O_DS, O_DC, and O_DO_D pairs of sites belonging to distinct DMSO molecules (Fig. 2). The line styles and the corresponding mole fractions of DMSO are as indicated. The thick solid lines are for neat DMSO. At the outset, one can notice that the overall distribution of DMSO is relatively little affected by addition of water into the system. The $g_{SS}(r)$ distribution function, for instance, which measures approximately the distribution of the center of masses of DMSO, remains essentially unaffected even for DMSO concentrations as low as 13%. Similar behavior is also found for $g_{\text{CC}}(r)$ (not shown) and other DMSO site-site functions. One also notices that the peak heights decrease with decreasing x_D, a result of DMSO becoming increasingly scarce as water is added into the system. The most

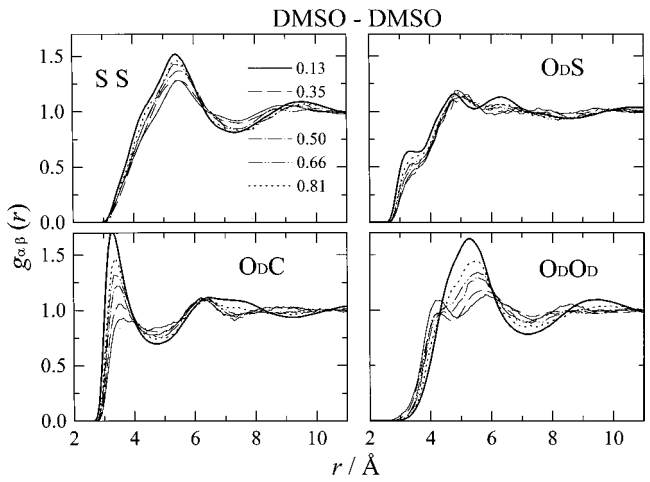

FIG. 2. DMSO–DMSO pair distribution functions $g_{\alpha\beta}(r)$ involving the SS, O_DS, O_DC, and O_DO_D pairs for mixtures of different compositions.

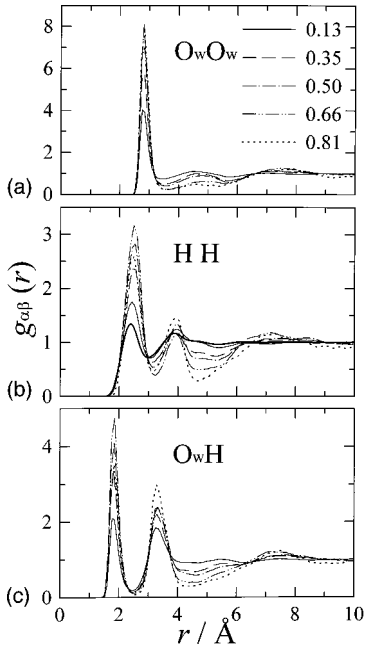

FIG. 3. Water–water pair distribution functions for mixtures of different composition.

substantial changes occur in g_{OC} and g_{OO}, which exhibit a considerable decrease in the first peak height as the water content increases.

Interestingly, the left flank of the first peak of g_{OO} moves to lower values of r, indicating that addition of water is capable of promoting an effective attractive interaction between the oxygen atoms of DMSO relative to the pure liquid. The O_DO_D data present a distinctive shoulder around 4.3 Å at several compositions. This feature of the O_DO_D pair distribution has also been noticed by Soper and Luzar,[8] who point to the possibility of an association between DMSO molecules reminiscent of that found in the crystalline phase of pure DMSO, and by Vaisman and Berkowitz,[7] who considered the left shift of the O_DO_D pair distribution as evidence of hydrophobic association of DMSO. We shall see below that this effect is actually promoted by the water molecules in a very specific way through H-bonding with DMSO oxygen.

Further inspection of Fig. 2 reveals that the diffusive peaks in the g_{OS} and g_{OC} for pure DMSO (thick lines) located around 6.5 and 7.5 Å, respectively, are practically washed away when water is present at mole fractions larger than 20% or so, indicating that the vicinity of the oxygen atom of DMSO is being gradually replaced by water species sites. These results indicate to us that when water is added into a sample of DMSO, its molecules tend to first occupy available interstitial space within the structure of DMSO, and that this process is mainly driven by the strong electrostatic attraction between DMSO's oxygen and water's hydrogen.

B. Water-water pair distributions

Let us now investigate how the structure of water changes upon mixing with DMSO. The three site-site functions for water are shown in Fig. 3, where the lines are labeled according to the mole fraction x_D of DMSO, as in Fig. 2. Results for neat water are shown only for the pair HH (thick line, Fig. 3(b)). The first peak heights in the water–water distribution functions increase sharply with decreasing water content, indicating that the water molecules in the mixture become highly correlated with each other despite the reduction in the average local concentration of water. This means that the potential of mean force between water molecules is enhanced in the presence of DMSO molecules.[6] Such behavior is contrasted with that presented by DMSO, where mixtures with smaller fractions of DMSO present lower peaks in the DMSO–DMSO pair correlations. This feature has been found in many binary aqueous mixtures, as discussed elsewhere.[11] As already mentioned, in the specific case of aqueous DMSO mixtures, it has been recently shown[8] that such enhanced water–water correlations are not due to hydrophobic hydration of the water molecules around DMSO's methyl groups, but a result of the strong H-bonding between crossed species. Obviously, the enhancement of the first peak heights in the water–water pair correlations has to subside as one approaches the limit of pure water. Indeed, Fig. 3 shows that at $x_D=0.81$, the first peaks in g_{HH} and g_{OH} start to decrease.

Previous simulation results[5b,6] and neutron diffraction data[5] have shown that the average tetrahedral coordination of water is preserved for concentrations as high as 35% mole DMSO (the most concentrated solution considered there). Such tetrahedral order is most easily characterized by the positions $r_1=2.8$ and $r_2=4.6$ Å of the first and second peaks of O_WO_W pair distribution, which roughly satisfy the tetrahedral[21] relation $r_2=2\sqrt{2/3}\,r_1$. Our O_WO_W function depicted in Fig. 3(a) shows that this tetrahedral order is still clearly defined even for the equimolar mixture, but is lost for more concentrated solutions. The preservation of the tetrahedral order of water in mixtures with $x_D \leqslant 0.5$ is partly due to the fact that at these compositions, DMSO oxygen makes on the average two H-bonds with water and, like in pure water, the angle between these two H-bonds is nearly tetrahedral (see below).[5,6]

Figure 3(b) and 3(c) also show that the g_{HH} and g_{OH} functions develop pronounced peaks and valleys at short dis-

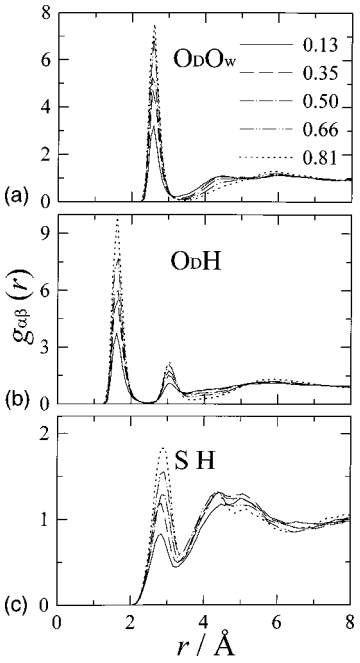

FIG. 4. DMSO–water pair distribution functions for O_DO_W, O_DH, and SH pairs for mixtures with different compositions.

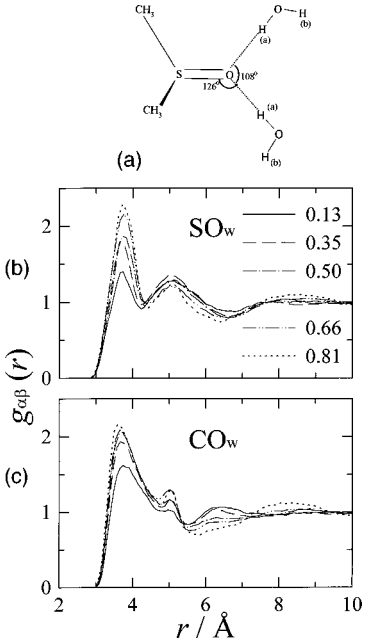

FIG. 5. Same as Fig. 4 for the pairs SO_W and CO_W. (a) represents the nearly tetrahedral order of the 1DMSO-2water molecular aggregates.

tances and also a broad minimum in the range 4–6.5 Å with increasing concentration of DMSO. The first two peaks of both these functions are well-known characteristics of nearest neighboring molecules in pure water. Thus one sees that the typical geometry of water dimers found in the neat liquid[22] is at least partially sustained in the mixtures even for water mole fractions as low as 20% or so ($x_D = 0.81$).

C. Water-DMSO pair distributions

Details about the average relative disposition between DMSO and water molecules can be extracted from the $g_{\alpha\beta}(r)$ functions involving the site pairs O_DO_W, O_DH, SH, SO_W, and CO_W (Figs. 4 and 5). The line styles and the corresponding mole fractions of DMSO are as indicated. The presence of sharp peaks in the O_DO_W and O_DH distributions at 2.6 and 1.6 Å , respectively, is indicative of the formation of H-bonds between DMSO and water and that these H-bonds are, on the average, collinear with the H–O bond of water. The average DMSO–water H-bond distance (1.6 Å) is somewhat smaller than the average water–water H-bond length (1.8 Å), which means that water may form stronger H-bonds with DMSO than with water itself. The first and second peaks of the O_DH distribution are separated by a ''population gap'' between 2 and 3 Å, indicating that the H-bonds formed between DMSO and water should be relatively rigid ones, with not much room for bending. However, rotations of nonbonded hydrogens [for instance, the H(b) atoms on Fig. 5] around the axis defined by O_D...H–O_W may, in principle, occur with low energy costs.

The average relative disposition of neighboring DMSO and water molecules in the mixtures is conveniently represented by the schematic on top of Fig. 5, where the dashed lines represent H-bonds. The angle of 126° between S═O...H(a) (or equivalently between S═O...O_W) is found by elementary geometry considering the first peaks of the O_DO_W and SH (or SO_W) pair distributions. On average, the atoms shown are all in the same plane, except for the methyls and the hydrogens labeled (b), which may loosely rotate around the axis of the water–DMSO H-bond if they are not themselves bonded to other neighboring water or DMSO molecules (not shown). The angle between the two H-bonds shown (108°) is thus close to the tetrahedral angle. This implies that average distance between the hydrogens H(a) is about 2.7 Å (roughly the same found for pure water), which agrees with the position of the first peak of the HH distribution [Fig. 3(b)] for all mixtures studied. The hydrogen atoms (b), whether rotated or not, contribute to the well-defined second peak of the O_DH pair distribution [Fig. 4(b)] at $r = 3.0$ Å, as well as to the hump located near 4.4 Å in the SH distribution function [Fig. 4(c)]. The position of the broad first peak of the CO_W pair distribution [Fig. 5(c) panel] is also consistent with this schematic representation of the local structure.

The picture emerging from these data is in complete agreement with other analyses,[5,6] namely, that by adding DMSO into water, one gradually replaces an H-bond accepting water molecule by a DMSO, keeping the local tetrahedral coordination nearly unchanged. There are, however, two aspects worth pointing out in connection with this suggested local structure. First, the schematic indicates a DMSO molecule H-bonded to two water molecules. An analysis of the H-bond distribution, using well-known geometrical criteria[6,9,11] to establish whether a pair of molecules is H-bonded or not (see below), shows that on the average DMSO makes two H-bonds with water for mixtures with DMSO mole fractions not larger that 50%, but for DMSO richer mixtures there is simply not enough water available in the system, and hence the average number of H-bonds for each bonded DMSO molecule drops to one (see below).

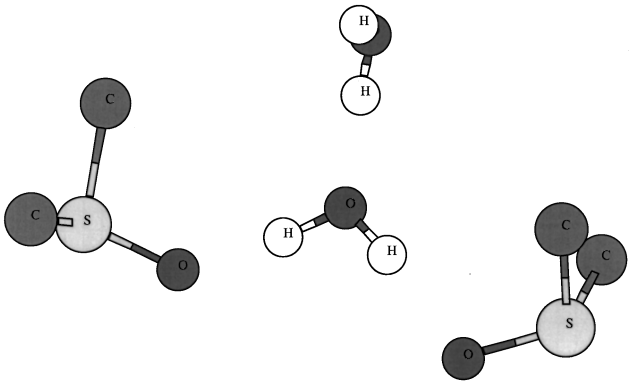

FIG. 6. Snapshot from an actual MD configuration at 81% DMSO showing a typical 2DMSO-1water aggregate with a second water molecule (out of the plane of the paper) acting as an H-bond donor to the central water molecule which in turn is H-bonded to the two DMSO.

Thus, in DMSO-rich mixtures, the average coordination number of water oxygens for separations around 4.5 Å (the distance between the two O_W shown in the schematic of Fig. 5) should drop considerably. This is well borne out by the O_WO_W pair distribution, which shows loss of tetrahedral order for mixtures with more than 50% of DMSO [Fig. 3(a)]. Second, the development with increasing x_D of the structures located about 5.1 and 5.0 Å in the SO_W and CO_W (Fig. 5) pair distributions, respectively, cannot be accounted for by the average geometry of the water–DMSO aggregate depicted in Fig. 5. Furthermore, the broad peak in the SH pair distribution between 4 and 6 Å presents two resolved maxima centered near 4.4 and 5.1 Å. The first of these has contributions from SH(b) pairs, according to the schematic of Fig. 5, as discussed above. The presence of a maximum at 5.1 Å, however, indicates that another water molecule must be in the vicinity and that its oxygen site and one of its hydrogens are, on the average, nearly equidistant from DMSO's S atom (both SO_W and SH present a peak at 5.1 Å).

These features, along with the fact that the typical water dimer is preserved for mixtures with DMSO mole fractions as high as 81%, have led us to suspect that some sort of well-defined structure, other than the known 1DMSO-2water aggregates, involving a number of DMSO and water molecules, should be found in mixtures rich in DMSO. In particular, the existence of 2DMSO-1water aggregates has been suggested by Tokuhiro *et al.*[23] based on the composition dependence of the NMR chemical shift. Indeed, molecular aggregates like the one shown in Fig. 6 can be clearly identified from stereoplots of the molecular trajectories for the mixture with 81% DMSO. The picture (taken from an actual MD configuration of this mixture) shows a central water molecule flanked by two DMSO molecules, H-bonded to each of its hydrogen atoms, and a second water molecule (out of the plane of the sheet) which is also H-bonded to it in a configuration resembling the typical nearest-neighbor disposition in pure water.[22] The angle defined by the average positions of S═O...H–O_W, as well as the distances between neighboring water and DMSO, are all in accord with our discussion above in connection with the schematic of Fig. 5 and also of Fig. 6. The site-site separations between DMSO and the second water molecule are consistent with the maxima around 5 Å found in the pair distributions involving the SH, SO_W, and CO_W (Figs. 4 and 5). It should be pointed out that this structure is surrounded mostly by other DMSO molecules and that there is a considerable fraction of water molecules which are H-bonded to only one DMSO and to another water. Interestingly, the average distance, 4.3 Å, between the oxygen atoms of DMSO in the structure shown in Fig. 6, is precisely the location of the shoulder we find in the O_DO_D pair distribution function (Fig. 2). Thus the features of the first peak in the O_DO_D pair distribution which appear in the mixtures can be thought of as a hydrophilic rather than hydrophobic association of DMSO. It is also implicit in Fig. 6 that the addition of water into DMSO may introduce a larger degree of antiparallel alignment of dipoles between neighboring DMSO molecules than that found in the pure liquid.[12] A calculation of the $h^{110}(r)$ dipolar symmetry projection for DMSO molecules in these mixtures is entirely consistent with that.[24] This and other orientational properties, as well as more detailed analyses of the H-bonding distribution for these mixtures, warrant further investigation. It is, nevertheless, reassuring to notice that this feature in the O_DO_D pair distribution function is also seen in the neutron scattering data.[8]

D. Distribution of H-bonds

Our discussion so far has been focused on determining the average geometry of the molecular aggregates that the several pair distribution functions obtained from MD seem to point to in these mixtures. The structures depicted in Figs. 5(a) and 6 are not mutually exclusive, but actually complementary to each other as they differ mainly in the number of H-bonds DMSO is sharing with water. The structure of Fig. 5, appropriately surrounded by additional water molecules, seems to be representative of water-rich mixtures, while that of Fig. 6 (surrounded by other DMSO molecules) should be more representative of DMSO-rich mixtures. As the water-to-DMSO ratio is changed in the mixture, one type of structure prevails over the other. In order to quantify this, we have determined the distribution of H-bonds for each mixture, where a pair of molecules is considered as being H-bonded if the relative disposition is such that the O...O distance is smaller than 3.5 Å, the O...H distance smaller than 2.6 Å, and the angle $\angle$H–O...O is no greater than 30°. This geometrical criterion is the same used in water-acetone and water–methanol mixtures,[25] but differs slightly from the one employed by Luzar and Chandler,[6] which in turn differs from Vaisman and Berkowitz's.[7] We find that using different criteria yields slightly different H-bonding distribution, but the qualitative features we discuss below remain unaltered. The distribution of H-bonds has been calculated in terms of the fraction of water molecules making a certain number of bonds with water itself [Fig. 7(a)] and with DMSO [Fig. 7(b)]. Also of interest is the fraction of DMSO making a given number of H-bonds to water [Fig. 7(c)].

At our smallest fraction of DMSO, the water–water H-bond distribution resembles that of pure water, with maximum around three or four H-bonds per water molecule on the average. As the content of DMSO increases, the peak of the distribution gradually shifts to lower number of bonds, a

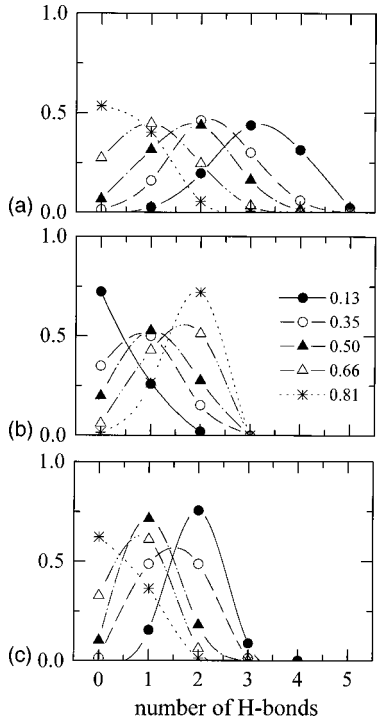

FIG. 7. Distribution of H-bonds for mixtures of different compositions. (a) depicts the fractions of water making H-bonds to water itself. (b) depicts the fractions of water making H-bonds to DMSO molecules. (c) shows the fractions of DMSO molecules making H-bonds with water. The lines are drawn as a guide to the eye.

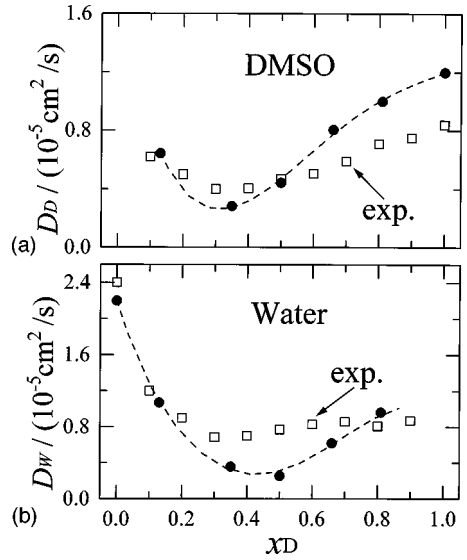

FIG. 8. Self-diffusion coefficients for water [(b) circles] and DMSO [(a) circles] as functions of composition. The open squares are experimental measurements taken from Ref. 27. The lines are drawn as guides.

result of the decreasing availability of water in the system and also of the competition for H-bonds from DMSO, which is a good H-bond acceptor. This is apparent in the data shown in Fig. 7(b) (fractions of water making H-bonds to DMSO), which show that the average number of H-bonds water makes with DMSO changes from one to two as x_D increases. At 81% DMSO, about half of the water molecules make one H-bond to another water [dotted line, Fig. 7(a)], while the other half are engaged in one (~20%) or two (~80%) H-bonds with DMSO [dotted line, Fig. 7(b)]. At low mole fractions of DMSO (e.g., 13%), the distribution for the fraction of DMSO making bonds with water [Fig. 7(c)] shows that most (~80%) DMSO is H-bonded to two water molecules. As the composition changes from low to high DMSO content, the distribution of H-bonds is intermediate between these two scenarios. This is in close agreement with our discussion above in connection with the local structures. It also is interesting to notice from Fig. 7(c) that at the lowest fraction of DMSO considered here, about 15% of the DMSO molecules make just one bond to water while about 8% of them are capable of accepting three hydrogen atoms, forming 1DMSO:3water H-bonded aggregates. Such aggregates are not unexpected in view of the resonant nature of the SO bond of DMSO, and have been experimentally observed in the solid phase[26] and also in other simulations in the liquid state.[6,7]

E. Diffusion coefficients and reorientational relaxation times

We conclude this section by presenting the results for some of the dynamical properties we obtained from the simulations. We start with the self-diffusion coefficients for each molecular species obtained from the mean-squared displacements, which are depicted in Fig. 8. Also shown are the experimental data (hollow squares) from Packer and Tomlinson.[27] Figure 8 shows that the molecular mobilities for each species change considerably with composition. At their respective minima, the simulated self-diffusion coefficients for water and DMSO are almost one order of magnitude smaller than in the pure liquids. DMSO molecules are slowest at about 33% DMSO, while water is slowest in the equimolar mixture. The behavior of the average diffusion coefficient with composition (not shown) parallels that of the experimental viscosity,[1] that is, both present extremum at about 33% DMSO. Overall, we find good agreement between the simulated and experimental self-diffusion coefficients, especially at low concentrations of DMSO. For mixtures with $x_D > 0.5$ there are larger discrepancies for D_D, which we believe are mostly due to the fact that model $P2$ exhibits somewhat faster dynamics than real DMSO.[12] Around the equimolar composition, the simulated self-diffusion coefficient for water is considerably smaller than the experimental values. This again indicates that the molecular interactions in the mixture may be overestimated.

Also of interest are the single-particle reorientational relaxation time, τ_2, for water and DMSO, which are shown in Fig. 9. The correlation times were calculated by integrating the correlation functions $C_2(t) = \langle P_2[\hat{u}(t) \cdot \hat{u}(0)] \rangle$, where P_2 is a Legendre polynomial and $\hat{u}$ a molecule-fixed unit vector. The vectors of interest are the OH bond for water and the dipole vector for DMSO. The trend with composition exhibited by the relaxation times parallels that of the self-diffusion coefficients, with DMSO presenting slowest reorientational dynamics at $x_D \approx 0.35$ while water is slowest around equimolar composition. The simulated data show that the dynamics of one species is slowed down upon addition of the other and vice-versa due to the molecular association

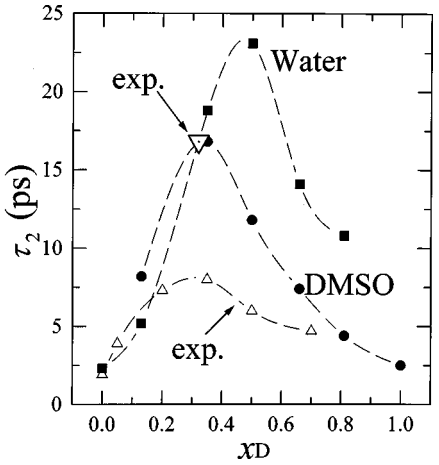

FIG. 9. Single-particle relaxation times for DMSO (dipole vector) and water (OH bond) as functions of composition. Experimental estimates for water's relaxation times according to Ref. 28(a) are shown by upright triangles. The large upside down triangle is experimental data from Ref. 28(b). The lines are drawn as a guide to the eye.

between cross species. Except at low DMSO mole fractions, water seems to be somewhat more sluggish than DMSO in the mixture. At $x_D \approx 0.35$, both DMSO and water present similar relaxation times, thus suggesting that some of the molecular aggregates may rotate together in these mixtures. This point warrants further investigation.

Figure 9 also shows the NMR relaxation times for water from Gordalla and Zeidler[28(a)] (upright triangles). For diluted solutions the agreement between simulated and experimental data is very good, but for DMSO concentrations larger than ~40%, the simulated water relaxation times are considerably higher than the experimental ones. We believe the reasons for that are twofold: First, there is overall indication from the present simulations that the interactions between water and DMSO are overestimated, which thus renders the system dynamically stiffer than it should. Second, and more importantly, the experimental τ_2 relaxation times are obtained from the spin-lattice relaxation times T_1 under several simplifying assumptions, including of isotropic reorientation of water molecules, which as pointed out by Gordalla and Zeidler,[28(a)] may not be realistic for concentrated solutions if long-lived complexes are present in the mixture. In a later and more elaborate experiment,[28(b)] the same authors show that the water correlation time at $x_D = 0.32$ is actually 16.8 instead of 8 ps as given in their previous work [Ref. 28(a)]. These experimental data are depicted in Fig. 9 by a large upside down triangle. It is stimulating to see that the agreement with our simulation at this composition is perfect. Although there are no actual experimental data at other compositions using this more reliable procedure,[28(b)] it is argued in Ref. 28(b) that this increase in the correlation time arises when the intramolecular OH bond length is not kept fixed at the pure water value as in Ref. 28(a), but recalculated from their measurements on the mixture.[28(b)] Thus, the experimental correlation times are expected to increase from their earlier values[28(a)] (Fig. 9, upright triangles) by a composition dependent factor which should increase from roughly one at small DMSO concentrations, being nearly two around 30% DMSO, and possibly larger for some DMSO richer mixture. In view of this, we may consider satisfactory the overall agreement between the simulated and experimental water correlation times.

As for the reorientational times for DMSO molecules in the mixture, we find it hard to make a meaningful comparison with experimental estimates. Although several independent measurements present similar values for DMSO's T_1 relaxation times,[23,27–29] the approximations leading to estimates for DMSO's τ_2 are highly questionable.[23,28] Regarding the qualitative aspect, however, both the simulated reorientational time τ_2 and the experimental spin-lattice relaxation parameter $1/T_1$ for DMSO go through a maximum around $x_D \approx 0.35$.

IV. CONCLUDING REMARKS

In this work we have presented an MD simulation study of the local structures, the H-bond distribution, and some dynamical properties of DMSO–water mixtures over the entire composition range. Our analysis has shown that two leading types of molecular aggregates coexist in these mixtures: One formed by a DMSO H-bonded to two water molecules in a nearly tetrahedral arrangement [top of Fig. 5(a)], which had already been identified in previous works through computer simulations and neutron scattering, and another consisting of a central water molecule with one DMSO H-bonded to each of its hydrogen atoms. A fraction of this type of aggregate also presents a second water molecule acting as an H-bond donor to the central water (Fig. 6). At high water-to-DMSO ratios, 1DMSO-2water aggregates are more abundant than 2DMSO-1water aggregates, whereas at low water-to-DMSO ratios the opposite is true. The distribution of H-bonds indicates that at intermediate compositions both types of aggregates are nearly equally abundant. It would not be surprising to find that at intermediate compositions these aggregates are interconnected in a persistent networklike fashion.

2DMSO-1water aggregates may not have as distinctive an impact on the thermodynamics, dielectric constant, viscosity, or dielectric relaxation times[30] of these solutions as that attributed to 1DMSO-2water complexes, but may be manifested in physicochemical quantities sensitive to the short-time dynamics. For instance, the fast librational motion of water molecules in DMSO-rich mixtures is expected to deviate considerably from that found in pure water due to the fact that in DMSO-rich mixtures water should be mostly found in the form of 2DMSO-1water aggregates like the one shown in Fig. 6, where the hydrogen atoms are tightly bonded to massive DMSO molecules. In a recent work,[31] we have shown that, according to the simulations, the far infrared absorption coefficient of DMSO-rich mixtures presents a distinctive band shape at the librational frequencies of water due to 2DMSO-1water aggregates, thus suggesting that far infrared spectroscopy could be a promising technique to unambiguously detect the presence of these aggregates experimentally. Theoretical investigation of these and other properties of DMSO–water mixtures under the light of the present local structures is currently underway.[24]

Finally, we would like to close this paper with a brief comment on the behavior we find for DMSO–water mixtures compared with that exhibited by other simulations of H-bonded mixtures. In particular, we would like to pay close attention to water–methanol and water–acetone mixtures.[25] The former because it is an example of a mixture where both constituents are H-bonding liquids on their own, thus contrasting with the present case, and the latter because of the similarity between acetone and DMSO molecules. In terms of the thermodynamic behavior, all three mixtures present exothermic heat of mixing, but in our mixtures the minimum lies around the equimolar composition, and this is in apparent contradiction with experimental measurements, as already discussed. In terms of the H-bonding distribution, the enhanced acceptor character of methanol or acetone is a dominant feature only at low concentrations of these species,[25] while the strong acceptor character of DMSO is manifested throughout the entire composition range. Unquestionably, the most striking difference between DMSO–water and the other mixtures is the much stronger associative character of the former. DMSO-water aggregates of well-defined structure and stoichiometry are identified over the whole composition range in contrast with the other mixtures where there is no evidence of such complexes. A direct consequence of that is the drastic slowing down of the dynamics of water molecules upon addition of DMSO and vice-versa. Retardation in the diffusion of water, methanol, and acetone upon mixing, as well as in some of the single-particle τ_2 reorientational correlation times, has been observed in the other mixtures[25] but the effects are noticeably milder than those we find for DMSO–water. A very revealing aspect of the relaxation times of DMSO–water mixtures shown in Fig. 9 is the presence of distinctive maxima between 30% and 50% DMSO, which points to the importance of the H-bond connectivity around these compositions in slowing the molecules down in comparison with the addition of the more sluggish DMSO component at all concentrations studied. This behavior is contrasted with that found by Ladanyi and Skaf[32] for methanol–water mixtures, where the effects of the H-bond connectivity of the equimolar mixture on the dipolar relaxation do not surpass those due to a high concentration of the ''heavier'' methanol component.

ACKNOWLEDGMENTS

This work has been supported by the Brazilian agencies FAPESP (Grant No. 95/9508-7) and CNPq. Partial support has been provided by the Research Foundation of the State University of Campinas (FAEP). I.B. gratefully acknowledges CNPq for a graduate research fellowship.

[1] M. G. Cowie and P. M. Toporowski, Can. J. Chem. **39**, 224 (1964).
[2] F. Fox and K. P. Whittingham, J. Chem. Soc., Faraday Trans. 1 **71**, 1407 (1975).
[3] H. L. Clever and S. Pigott, J. Chem. Thermodyn. **3**, 221 (1971).
[4] See also, A. Luzar, J. Mol. Liq. **46**, 221 (1990).
[5] (a) A. K. Soper and A. Luzar, J. Chem. Phys. **97**, 1320 (1992); (b) A. K. Soper, A. Luzar, and D. Chandler, *ibid.* **99**, 6836 (1993).
[6] A. Luzar and D. Chandler, J. Chem. Phys. **98**, 8160 (1993).
[7] I. I. Vaisman and M. L. Berkowitz, J. Am. Chem. Soc. **114**, 7889 (1992).
[8] A. K. Soper and A. Luzar, J. Phys. Chem. **100**, 1357 (1996).
[9] A. Luzar, Faraday Discuss. **103**, 29 (1996).
[10] H. J. C. Berendsen, J. R. Grigera, and T. P. Straastma, J. Phys. Chem. **91**, 6269 (1987).
[11] B. M. Ladanyi and M. S. Skaf, Annu. Rev. Phys. Chem. **44**, 335 (1993).
[12] (a) M. S. Skaf, Mol. Phys. **90**, 25 (1997); (b) J. Chem. Phys. **107**, 7996 (1997).
[13] B. G. Rao and U. C. Singh, J. Am. Chem. Soc. **112**, 3803 (1990).
[14] W. L. Jörgensen, unpublished; see Y.-J. Zheng and R. L. Ornstein, J. Am. Chem. Soc. **118**, 4175 (1996), Ref. 18.
[15] H. Liu, F. Müller-Plathe, and W. F. van Gunsteren, J. Am. Chem. Soc. **117**, 4363 (1995).
[16] (a) S. W. De Leeuw, J. M. Perram, and E. R. Smith, Annu. Rev. Phys. Chem. **37**, 245 (1986); (b) Proc. R. Soc. London, Ser. A **373**, 27 (1980); (c) **373**, 57 (1980).
[17] (a) M. P. Allen and D. J. Tildesley, *Computer Simulation of Liquids* (Clarendon, Oxford, 1987); (b) R. W. Hockney, Methods Comput. Phys. **9**, 136 (1970).
[18] G. Ciccotti and J.-P. Ryckaert, Comput. Phys. Rep. **4**, 345 (1986).
[19] T. B. Douglas, J. Am. Chem. Soc. **70**, 2001 (1948).
[20] A. Luzar, J. Chem. Phys. **91**, 3603 (1989).
[21] P. J. Rossky, Annu. Rev. Phys. Chem. **36**, 321 (1985).
[22] (a) A. K. Soper, F. Bruni, and M. A. Ricci, J. Chem. Phys. **106**, 247 (1997); (b) A. K. Soper, J. Phys.: Condens. Matter **9**, 2717 (1997); (c) J. Dore, in *Molecular Liquids: New Perspectives in Physics and Chemistry*, edited by J. J. Teixeira-Dias (Kluwer, Dordrecht, 1992).
[23] T. Tokuhiro, L. Menafra, and H. H. Szmant, J. Chem. Phys. **61**, 2275 (1974).
[24] I. A. Borin and M. S. Skaf (in preparation).
[25] M. Ferrario, M. Haughney, I. MacDonald, and M. L. Klein, J. Chem. Phys. **93**, 5156 (1990).
[26] D. H. Rasmussen and A. P. Mackenzie, Nature (London) **220**, 1315 (1968).
[27] K. J. Packer and D. J. Tomlinson, Trans. Faraday Soc. **67**, 1302 (1971).
[28] (a) B. C. Gordalla and M. D. Zeidler, Mol. Phys. **59**, 817 (1986); (b) **74**, 975 (1991).
[29] E. S. Baker and J. Jonas, J. Phys. Chem. **89**, 1730 (1985).
[30] U. Kaatze, R. Pottel, and M. Schäfer, J. Phys. Chem. **93**, 5623 (1989).
[31] I. A. Borin and M. S. Skaf, Chem. Phys. Lett. **296**, 125 (1998).
[32] B. M. Ladanyi and M. S. Skaf, J. Phys. Chem. **100**, 1368 (1996).